Journal of Interdisciplinary Mathematics
ISSN: 0972-0502 (Print), ISSN: 2169-012X (Online)
Vol. 28 (2025), No. 6, pp. 2339–2348
DOI : 10.47974/JIM-2376

Solution of nonlinear differential equations for hybrid nanofluid flow over stretching/shrinking permeable sheets with heat generation and stability analysis

D. B. Lakshmikantha [@]
Department of Mathematics
Vivekananda Institute of Technology
Bengaluru
Karnataka
India

N. Raveendra [†]
Department of Mathematics
ACS College of Engineering
Bengaluru
Karnataka
India

D. V. Jayalakshamamma [§]
Department of Mathematics
Vemana Institute of Technology
Bengaluru
Karnataka
India

M. C. Kemparaju [‡]
Department of Mathematics
Jyothy Institute of Technology
Bengaluru
Karnataka
India

[@] *E-mail:* lakshmikanthjeeva@gmail.com
[†] *E-mail:* r.ravi1505@gmail.com
[§] *E-mail:* jaya.dvj@gmail.com
[‡] *E-mail:* kemparajumc@gmail.com

D. V. Chandrashekar *
Department of Mathematics
Vivekananda Institute of Technology
Bengaluru
Karnataka
India

Abstract

The paper discusses the effects of a hybrid nanofluid that is magnetically driven in presence of the heat produced on a permeable sheet that rattles the exponential elongation or contraction. The hybrid nanofluid comprises copper nanoparticles and alumina which are dissolved in the carrier fluid, water. The governing equation is then transformed into a simpler (mathematically) one with similarity transformation. MATLAB acts as the solver of the numbers and the bpvc4 is involved in getting the twin answers. Reaction of significant variables to the predominant physical factors and flow characteristics is discussed and explicated by graphical shows. Rather, stability analysis and the resultant results can be used to conclude that the first one, not the other solution is relevant physically. As the proportion of the copper nanoparticle is enhanced by increasing the volume, lthe lcoefficient lof lfriction lrises land lthe llocal lNusselt lnumber lrises las lwell.

Subject Classification (2010): *94A60, 20C05, 20C07.*

Keywords: *Copper nanoparticles, Hybrid nanofluid, Nusselt number, Skin friction, Slip condition, Suction parameter.*

1. Introduction

Diversity in mixing up various nanoparticles in a standard fluid creates much better nanofluids that are more stable to transfer heat. They occur in cooling systems, in solar collectors and are used in certain medical apparatus. Conversely, other aspects such as the cost of the process, the generation of sediment and utilization of toxic components have to be considered. This transformation in fluid flow, when states of stretching and shrinking are involved, is a subject of common study in the industry, primarily to examine heat and mass transfer, given that often instability becomes highly significant in order to avoid the procedure of flow separation occurring on the shrinking areas.

2. Literature Review

The authors of [1] have made known that accidental nanofluids can be used to enhance the establishment of heat in corrugated enclosures. The authors of [2] and [5] have studied the various ways through which the said materials can be applied, how such materials can be prepared, and have enumerated some of the

* *E-mail:* **dvchandru@gmail.com (Corresponding Author)**

already existing research questions within the area. The flow of nanofluids was explored due to the impact of magnetic fields and at a high temperature by the authors of [3]. The authors of [4] presented a research work over a porous surface which is expanding or contracting in the slip conditions. The authors of [6] conveyed a set of articles which evaluate numerical simulation of suctioning CuAl2O3/water nanofluid. The performance and thermal properties of hybrid nanofluid had been discussed by authors of [8] and [7]. The authors of [9] has emphasized the fact that slip may contribute to the hybrid nanofluids which are under the rotating motion. One of the studies by the authors of [10], investigated the stagnation flow of a MHD and heat generation. To examine the example of the flow of hybrid nanofluids towards the permeable sheet, the authors of [11] took into account the analytical and numerical study. The authors of [12] examined the question of wall slip along with the magnetic influence on blood stream. The authors of [13] narrowed down the research to a shrinking exponentially sheets, by using hybrid nanoparticles. The papers by [14] focused on the MHD mixed flow around the surfaces of different areas which were exposed to both radiative and suction influence. This included the nonlinear shortening of pages of research of the viscous dissipation of the writers of [15]. The authors of [16] talked about non-stabilizing forces of Cu5Al 2O mixing with water. The analysis of MHD flow due to a partial slip and radiation gives the results by the authors of [17]. The authors of [18] examined Ag nanoparticles with an aim to determine the slip flow properties over shrinking porous sheets.

3. Proposed Methodology

3.1 *Mathematical Formulation*

Let the surface velocity is symbolized by $S_u(x) = ce^{\frac{x}{L}}$ and $W_m(x) = W_0 e^{\frac{x}{2L}}$ symbolizes the wall mass transfer, with the suction is given by $W_0 < 0$ and $W_0 > 0$ is injection, $\lambda > 0$, $\lambda < 0$, and a motionless sheet described by $\lambda = 0$ symbolize stretching, pulling and a still surface, respectively. The temperature on the sheet is constant T_0 but varies at $T_w = T_\infty + T_0 e^{\frac{x}{2L}}$ [19]. Table 1 depicts the properties of hybrid nanofluid whereas Table 2 and Table 3 coveys about Thermo-physical properties and tabulation

$$\frac{\partial S}{\partial x} + \frac{\partial W}{\partial y} = 0 \tag{1}$$

$$S\frac{\partial y}{\partial x} + W\frac{\partial y}{\partial x} = \frac{\mu_{hnf}}{\rho_{hnf}}\frac{\partial^2 S}{\partial y^2} - \frac{\sigma B_0^2}{\rho} S \tag{2}$$

$$S\frac{\partial T}{\partial x} + W\frac{\partial T}{\partial y} = \frac{k_{hnf}}{(\rho C_p)_{hnf}}\frac{\partial^2 T}{\partial y^2} + \frac{q}{(\rho C_p)_{hnf}}(T - T_\infty) \tag{3}$$

$$S = S_u(x)\lambda + A_1\frac{\mu_{hnf}}{\rho_{hnf}}\frac{\partial S}{\partial y}, W = W_m, T = T_w(x) + B_1\frac{\partial T}{\partial x}\ at\ y = 0\ S \to 0,$$
$$T \to T_\infty\ as\ y \to \infty \,\} \tag{4}$$

Table 1

Properties of Hybrid nanofluid

Properties	Hybrid nanofluid Correlation
Density	$\rho_{hnf} = \rho_{s1}\phi_{s1} + \rho_{s2}\phi_{s2} + \rho_f(1-\phi_{hnf})\ where\ \phi_{hnf} = \phi_{s1} + \phi_{s2}$
Heat Capacity	$(\rho C_p)_{hnf} = (\rho C_p)_{s1}\phi_{s1} + (\rho C_p)_{s2}\phi_{s2} + (\rho C_p)_f(1-\phi_{hnf})$
Dynamic Viscosity	$\frac{\mu_{hnf}}{\mu_f} = \frac{1}{(1-\phi_{hnf})^{2.5}}$
Thermal Conductivity	$\frac{k_{hnf}}{k_f} = \left[\frac{2k_f + \left(\frac{\phi_{s1}k_{s1}+\phi_{s2}k_{s2}}{\phi_{hnf}}\right) + 2(\phi_{s1}k_{s1}+\phi_{s2}k_{s2}) - 2\phi_{hnf}k_f}{2k_f - (\phi_{s1}k_{s1}+\phi_{s2}k_{s2}) + \left(\frac{\phi_{s1}k_{s1}+\phi_{s2}k_{s2}}{\phi_{hnf}}\right) + \phi_{hnf}k_f}\right]$

Table 2

Thermo -physical properties

Physical Properties	Water	Al_2O_3	Cu
$\rho(kg/m^3)$	997.1	3970	8933
$C_p(J/kgK)$	4179	765	385
k(W/mK)	0.613	40	400

Table 3

Tabulation of $f''(0)$ & $'(0)$ for viscous fluid $(\phi_{s1} = \phi_{s2} = 0)$ when $Pr = 0.7, S = 3$ and $A = B = \beta = 0$ for the shrinking surface $(\lambda = -1)$

Author Name	$f''(0)$		$\theta'(0)$	
Ghosh and Mukhopadhyay	2.39082	- 0.97223	1.7712	0.84832
Hafidzuddin et al.	2.3908	- 0.9722	1.7712	0.8483
Waini et al.	2.390814	- 0.972247	1.771237	0.848316
Nur SyahirahWahid et al.	2.390813634	-0.972128	1.771237307	0.847748272
Present Results	2.390813636	-0.9721288	1.771237309	0.847748275

$$\varphi = e^{\frac{x}{2L}}\sqrt{2v_f Lcf(\eta)}, u = \frac{\partial\varphi}{\partial y}, v = \frac{\partial\varphi}{\partial x}, \theta(\eta) = \frac{T-T_\infty}{T_w-T_\infty}, \eta = ye^{x/2L}\sqrt{\frac{C}{2v_f L}} \qquad (5)$$

$$\left(\frac{\mu_{hnf}/\mu_f}{\rho_{hnf}/\rho_f}\right) f^{111} + ff^{11} - 2f^{1^2} - Mf'(\eta)\, l = 0 \qquad (6)$$

$$\frac{1}{P_r}\left(\frac{k_{hnf}}{k_f}\right)\theta^{11} + \frac{(\rho C_p)_{hnf}}{(\rho C_p)_f}(f\theta^1 - f^1\theta) + \beta\theta = 0 \qquad (7)$$

The transformed boundary conditions are [20]:

$$(0) = S, f^1(0) = \lambda + Af^{11}(0), \theta(0) = 1 + B\theta^1(0) f^1(\eta) \to 0,$$
$$f\ \theta(\eta) \to 0\ as\ \eta \to \infty\} \tag{8}$$

The coefficients for local skin friction (C_f) and the local Nusselt number N_{ux} are represented as [21]:

$$C_f = \frac{\mu_{hnf}}{\rho_f} \frac{1}{u^2{}_w} \left(\frac{\partial u}{\partial y}\right)_{y=0}, Nu_x = \frac{k_{hnf}}{k_f} \frac{-2L}{(T_w - T_\infty)} \left(\frac{\partial T}{\partial x}\right)_{y=0} \tag{9}$$

Then after the transform:

$$Re^{1/2}{}_x C_f = \left(\frac{\mu_{hnf}}{\mu_f}\right) f^{11}(0), Re^{-1/2}{}_x\ Nu_x = -\left(\frac{k_{hnf}}{k_f}\right) \theta^1(0) \tag{10}$$

Here, the local Reynolds number is symbolized by $Re_x = 2Lu_w/v_f$.

Table 4
Cfx Vs Lambda

Lambda	A = 0.2		A = 0.4		A = 0.6	
	Analysis -1	**Analysis - 2**	**Analysis - 1**	**Analysis - 2l**	**Analysis - 1**	**Analysis - 2**
1	-1.923775	-3.24669153	-1.389355	-2.385918096	-1.0915532	-1.90610302
0.5	-0.928311	-2.30099507	-0.6796242	-1.729719773	-0.5378836	-1.39812923
0	-5.700008	-1.44892802	-1.6895608	-1.115633648	-6E-08	-0.91104425
-0.5	0.8280545	-0.67971735	0.6385037	-0.527754158	0.51700833	-0.43013279
-0.8	1.2334522	-0.23304997	0.9934783	-0.16213515	0.81364911	-0.13060125
-1	1.489652	0.135603669	1.2132876	0.100185548	1.00383628	0.07958925
-1.1	1.5861082	0.332082299	1.3164585	0.240020045	1.09610746	0.18898346
-1.2	1.6608219	0.552957021	1.4139037	0.387351439	1.18614275	0.30179732
-1.3	1.6968767	0.809245995	1.5041632	0.543918426	1.27358261	0.4185066
-1.35	1.6968767	0.96252439				
-1.36	1.6929543	0.99666504				
-1.39	1.6709543	1.10872754				
-1.4	1.6586826	1.15235489	1.5849098	0.712268092	1.3579451	0.53968091
-1.42	1.6203496	1.24990875				
-1.43	1.5875276	1.34299449				
-1.44	1.523541	1.40977063				
-1.4419	1.4766923	1.45989390				
-1.5			1.6519574	0.896743998	1.4385604	0.66605501
-1.6			1.6959319	1.106835207	1.5144417	0.79865954
-1.65			1.7014426	1.229335693		
-1.7			1.6798886	1.379557092	1.5840115	0.93909744
-1.71			1.667753	1.417511003		
-1.72			1.6486881	1.462415925		
-1.73			1.6085623	1.52840979		
-1.7322			1.5776055	1.565060961		

Table 4 shows the comparison between cfx vs Lambda function.

3.2 *Flow Stability*

Since there are the available doubled solutions, analysis of flow stability is performed. Here the problem is taken as unsteady in the sense that the continuity equation (1) is retained but equation (2) and (3) are endowed with a time derivative.

$$u\frac{\partial u}{\partial x}+v\frac{\partial u}{\partial y}+\frac{\partial u}{\partial t}=\frac{\mu_{hnf}}{\rho_{hnf}}\frac{\partial^2 u}{\partial y^2} \tag{11}$$

$$u\frac{\partial T}{\partial x}+v\frac{\partial T}{\partial y}+\frac{\partial T}{\partial t}=\frac{k_{hnf}}{(\rho C_p)_{hnf}}\frac{\partial^2 T}{\partial y^2}+\frac{q}{\rho C_{p\,hnf}}(T-T_\infty) \tag{12}$$

Equation (11) and (12) can be re-written in the form of dimensionless variables in terms of time as follows:

$$\eta=ye^{\frac{x}{2L}}\sqrt{\frac{c}{2v_f L}}\,,\varphi=f(\eta,\tau)e^{\frac{x}{2L}}\sqrt{2v_f Lc},\theta(\eta,\tau)=\frac{T-T_\infty}{T_w-T_\infty},\tau=\frac{c}{2L}te^{\frac{x}{L}} \tag{13}$$

In this way, the transformation yields the resultant equations on its application:

$$\left(\frac{\mu_{hnf}/\mu_f}{\rho_{hnf}/\rho_f}\right)\frac{\partial^3 f}{\partial\eta^3}+\frac{\partial^2 f}{\partial\eta^2}f-2\left(\frac{\partial f}{\partial\eta}\right)^2-\frac{\partial^2 f}{\partial\eta\partial\tau}=0 \tag{14}$$

$$\frac{1}{P_r}\left(\frac{k_{hnf}}{k_f}\right)\frac{\partial^2\theta}{\partial\eta^2}+\frac{(\rho C_p)_{hnf}}{(\rho C_p)_f}\left(\frac{\partial\theta}{\partial\eta}f-\theta\frac{\partial f}{\partial\eta}-\left(\frac{\partial\theta}{\partial\tau}\right)\right)+\beta\theta=0 \tag{15}$$

Restricted to the condition

$$\left.\begin{aligned}&f(0,\tau)=S,\frac{\partial f}{\partial\eta}(0,\tau)=\ \lambda+A\frac{\partial^2 f}{\partial\eta^2}(0,\tau),\theta(0)=1+B\frac{\partial\theta}{\partial\eta}(0,\tau)\ \frac{\partial f}{\partial\eta}(\eta,\tau)\to\\&0,\theta(\eta,\tau)\to 0\ as\ \eta\to\infty\end{aligned}\right\} \tag{16}$$

This is then adequate to establish the perturbation equation to examine the perturbation solutions otherwise to test the similarity solutions.

$$\left.f(\eta,\tau)=f_0(\eta)+e^{-\gamma\tau}F(\eta)\ \theta(\eta,\tau)=\theta_0(\eta)+e^{-\gamma\tau}G(\eta)\right\} \tag{17}$$

By substituting eqn. (17) into eqns. (14)–(16) and adjusting t to 0, the decay of disturbances in equation (17) is determined, leading to the derivation of the corresponding linearized equations.

$$\left(\frac{\mu_{hnf}/\mu_f}{\rho_{hnf}/\rho_f}\right)F^{111}+{f_0}^{11}F+F^{11}f_0-4{f_0}^{1}F^1+\gamma F^1=0 \tag{18}$$

$$\frac{1}{P_r}\left(\frac{k_{hnf}}{k_f}\right)G^{11}+\frac{(\rho C_p)_{hnf}}{(\rho C_p)_f}\left({\theta_0}^1 f+G^1 f_0-\theta_0 F^1-G{f_0}^1+\gamma G\right)+\beta G=0 \tag{19}$$

Subject to the constraints

$$F(0)=0,F^1(0)=AF^{11}(0),G(0)=BG^1(0),F^1(\infty)\to 0,G(\infty)\to 0 \tag{20}$$

As conditions in equation (20) are equal to 0, it becomes obligatory to soften the condition $F'(\infty)\to 0$ and instead set $F''(0)=1$, so to obtain practical range of eigenvalues (γ). Being the indicators of the flow stability, the unknown γ, are found using a BVP4C solver. In case $\gamma>0$, it is claimed that the flow is stable, otherwise unstable.

4. Results and Analysis

The numerically provision of the options of eqns. (6) and (7) under the prerequisite of the limitations in eqn. (8) aids the usage of BVP4C solver in MATLAB.

To achieve good results, the cases of validity of initial solutions, sufficiency of tightness of the thickness of the cover layer, and values of another parameter should be selected correctly, and, with great caution, in the coding area of the solver. The protruding and contracting surfaces have been taken into consideration in the present paper. In light of a constant Pr=6.2, nanoparticle volume fraction of alumina should be maintained at a constant level at $\phi_{s1} = 0.01$.

Figure 1 and 2 present the arrangement of stretching and shrinking the sheet. As seen in Figure 3, temperature occurring because of B is as follows, and generation of heat could be seen to be having impact on thermal boundary layer. We see how the slip parameter A varies, with regard to skin friction. Such models can be used to define the influence of the basic physical factors on the transport of heat and the flow of the integration of hybrid nanofluids through the channels.

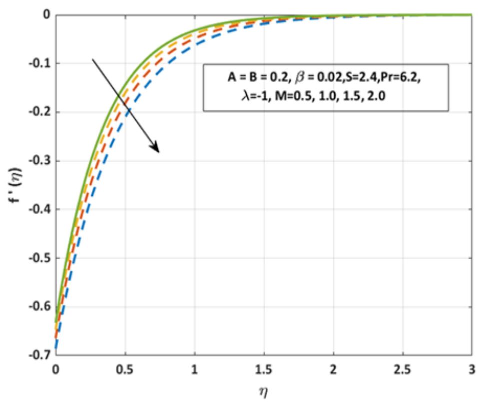

Figure 1
Nature of $f'(\eta)$ *with M*

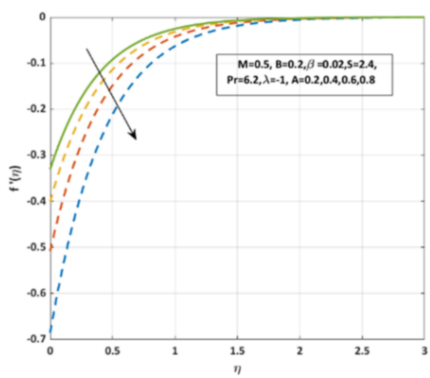

Figure 2
Behaviour of $f'(\eta)$ *with A*

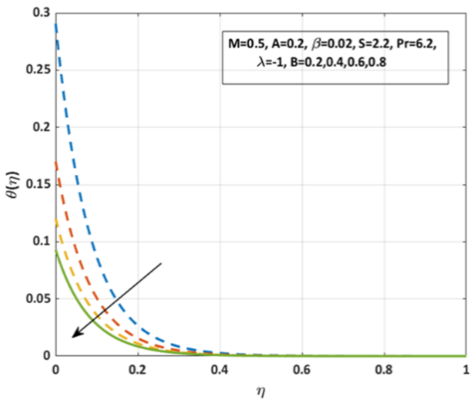

Figure 3
Influence of B on $\theta(\eta)$

5. Discussion and Conclusion

During the investigation Figure 1, Figure 2 and Figure 3 it is found it is found out that in the case where there is sufficient suction, there could be as many as two solutions of shrinking surface only that the first one was stable. The extension of the speed is reduced by the rise of the M (magnetic model) and the rise of the A (slip solution) reduces the skin friction. The height of suction and the quantity of the copper particles compose nanoparticles with the goal of getting a bigger friction coefficient. Furthermore, higher Nusselt number is also locally observed where the volume fraction of copper and suction flow is more and vice versa. Increased energy distribution due to the incorporation of copper and increased temperature in a compressor are negated by greater velocity slip, thermal slip and suction.

References

[1] B. Takabi and S. Salehi, Augmentation of the heat transfer performance of a sinusoidal corrugated enclosure by employing hybrid nanofluid, *Adv. Mech. Eng.*, vol. 6, pp. 147059, (2015).

[2] N.A.C. Sidik, I.M. Adamu, M.M. Jamil, G.H.R. Kefayati, R. Mamat, and G. Najafi, Recent progress on hybrid nanofluids in heat transfer applications: A comprehensive review, *Int. Commun. Heat Mass Transf.*, vol. 78, pp. 68–79, (2016).

[3] Z. Abbas, M. Naveed, and M. Sajid, Hydromagnetic slip flow of nanofluid over a curved stretching surface with heat generation and thermal radiation, *J. Mol. Liquids*, vol. 215, pp. 756–762, (2016).

[4] M.E.H. Hafidzuddin, R. Nazar, N.M. Arifin, and I. Pop, Boundary layer flow and heat transfer over a permeable exponentially stretching/shrinking sheet with generalized slip velocity, *JAFM*, vol. 9, pp. 2025–2036, (2016).

[5] N.A.C. Sidik, M.M. Jamil, W.M.A.A. Japar, and I.M. Adamu, A review on preparation methods, stability and applications of hybrid nanofluids, *Renew. Sustain. Energy Rev.*, vol. 80, pp. 1112–1122, (2017).

[6] S.P.A. Devi and S.S.U. Devi, Numerical investigation of hydromagnetic hybrid Cu–Al_2O_3/water nanofluid flow over a permeable stretching sheet with suction, *Int. J. Nonlinear Sci. Numer. Simul.*, vol. 17, pp. 249–257, (2016).

[7] L.S. Sundar, K.V. Sharma, M.K. Singh, and A.C.M. Sousa, Hybrid nanofluids preparation, thermal properties, heat transfer and friction factor—A review, *Renew. Sustain. Energy Rev.*, vol. 68, pp. 185–198, (2017).

[8] M.F. Nabil, W.H. Azmi, K.A. Hamid, N.N.M. Zawawi, G. Priyandoko, and R. Mamat, Thermo-physical properties of hybrid nanofluids and hybrid nanolubricants: A comprehensive review on performance, *Int. Commun. Heat Mass Transf.*, vol. 83, pp. 30–39, (2017).

[9] T. Hayat, S. Nadeem, and A.U. Khan, Rotating flow of Ag–CuO/H_2O hybrid nanofluid with radiation and partial slip boundary effects, *Eur. Phys. J. E*, vol. 41, pp. 75, (2018).

[10] R. Jusoh, R. Nazar, and I. Pop, Impact of heat generation/absorption on the unsteady magnetohydrodynamic stagnation point flow and heat transfer of nanofluids, HFF, vol. 30, pp. 557–574, (2019).

[11] E.H. Aly and I. Pop, MHD flow and heat transfer over a permeable stretching/shrinking sheet in a hybrid nanofluid with a convective boundary condition, HFF, vol. 29, pp. 3012–3038, (2019).

[12] J. Nandal, S. Kumari, and R. Rathee, The effect of slip velocity on unsteady peristalsis MHD blood flow through a constricted artery experiencing body acceleration, *Int. J. Appl. Mech. Eng.*, vol. 24, pp. 645–659, (2019).

[13] Waini, A. Ishak, and I. Pop, Hybrid nanofluid flow induced by an exponentially shrinking sheet, *Chin. J. Phys.*, (2019).

[14] U. Yashkun, K. Zaimi, N.A. Abu Bakar, A. Ishak, and I. Pop, MHD hybrid nanofluid flow over a permeable stretching/shrinking sheet with thermal radiation effect, HFF, (2020).

[15] L.A. Lund, Z. Omar, I. Khan, A.H. Seikh, E.-S.M. Sherif, and K.S. Nisar, Stability analysis and multiple solution of $Cu–Al_2O_3–H_2O$ nanofluid contains hybrid nanomaterials over a shrinking surface in the presence of viscous dissipation, *J. Mater. Res. Technol.*, vol. 9, pp. 421–432, (2020).

[16] N.A.L. Aladdin, N. Bachok, and I. Pop, $Cu–Al_2O_3$/water hybrid nanofluid flow over a permeable moving surface in presence of hydromagnetic and suction effects, *Alex. Eng. J.*, vol. 59, pp. 657–666, (2020).

[17] N.S. Wahid, N. Md Arifin, M. Turkyilmazoglu, M.E.H. Hafidzuddin, and N.A. Abd Rahmin, MHD hybrid $Cu–Al_2O_3$/water nanofluid flow with thermal radiation and partial slip past a permeable stretching surface: Analytical solution, *JNanoR,* vol. 64, pp. 75–91, (2020).

[18] S. Ghosh and S. Mukhopadhyay, Stability analysis for model-based study of nanofluid flow over an exponentially shrinking permeable sheet in presence of slip, *Neural Comput. Appl.,* vol. 32, pp. 7201–7211, (2020).

[19] A. A. Zaghrout, Y. S. A. Ali, and N. S. Abdelhameed, Epidemic model with nonlinear incidence rate and three-infectious individual classes. *Journal of Statistics and Management Systems,* vo. 25, no. 3, pp. 679-696, (2022).

[20] F. Diaba, and E. Cheremnikh, On asymptotic time for an evolution with non-local boundary condition, *Journal of Dynamical Systems and Geometric Theories,* vol. 4, no. 1, pp. 61-77, (2006).

[21] T. Körpinar, On inextensible flows of curves according to alternative moving frame, *Journal of Dynamical Systems and Geometric Theories,* vol. 15, no. 1, pp. 15-27, (2017).

Received December, 2024